Macrophages phagocytose nonopsonized silica particles using a unique microtubule-dependent pathway

Renée M. Gilberti* and David A. Knecht
Department of Molecular and Cell Biology, University of Connecticut, Storrs, CT 06269

ABSTRACT **Silica inhalation leads to the development of the chronic lung disease silicosis. Macrophages are killed by uptake of nonopsonized silica particles, and this is believed to play a critical role in the etiology of silicosis. However, the mechanism of nonopsonized-particle uptake is not well understood. We compared the molecular events associated with nonopsonized- and opsonized-particle phagocytosis. Both Rac and RhoA GTPases are activated upon nonopsonized-particle exposure, whereas opsonized particles activate either Rac or RhoA. All types of particles quickly generate a PI(3,4,5)P_3 and F-actin response at the particle attachment site. After formation of a phagosome, the events related to endolysosome-to-phagosome fusion do not significantly differ between the pathways. Inhibitors of tyrosine kinases, actin polymerization, and the phosphatidylinositol cascade prevent opsonized- and nonopsonized-particle uptake similarly. Inhibition of silica particle uptake prevents silica-induced cell death. Microtubule depolymerization abolished uptake of complement-opsonized and nonopsonized particles but not Ab-opsonized particles. Of interest, regrowth of microtubules allowed uptake of new nonopsonized particles but not ones bound to cells in the absence of microtubules. Although complement-mediated uptake requires macrophages to be PMA-primed, untreated cells phagocytose nonopsonized silica and latex. Thus it appears that nonopsonized-particle uptake is accomplished by a pathway with unique characteristics.**

Monitoring Editor
Paul Forscher
Yale University

Received: Aug 26, 2014
Revised: Nov 17, 2014
Accepted: Nov 20, 2014

INTRODUCTION

Alveolar macrophages play a major role in the immune response to foreign materials and pathogens that enter the body through the lungs (Gordon, 1995). Macrophages have cell surface receptors that have evolved to recognize antibodies or complement factors bound to pathogens or molecular signatures unique to pathogens (e.g., mannose polymers). The molecular mechanisms by which alveolar macrophages initially interact with inhaled environmental particles such as silica, however, are not clear. There is some evidence that scavenger receptors play a role in this process, particularly scavenger receptor-A (SR-A; Kobzik, 1995; Palecanda and Kobzik, 2001; Taylor *et al.*, 2005). However, SR-A receptors depend on negatively charged ligands, and nonopsonized-particle uptake by macrophages occurs regardless of particle charge (Gilberti *et al.*, 2008). Even when SR-A function is compromised by pretreatment with an SR-A inhibitor or use of a knockout mouse model, uptake of silica particles still occurs (Beamer and Holian, 2005; Hamilton *et al.*, 2006; Thakur *et al.*, 2009). These data suggest that SR-A receptors are only partially involved in phagocytosing silica particles.

Regardless of the mechanism of cell–particle interaction, macrophages rapidly internalize silica particles by phagocytosis. Silica particle uptake is lethal to macrophages, and it is this toxicity that is believed to be an important contributor to the development of silicosis, as suggested by in vivo and in vitro studies (Iyer *et al.*, 1996; Iyer and Holian, 1997; Hamilton, 2000; Chao *et al.*, 2001; Thibodeau *et al.*, 2003, 2004; Beamer and Holian, 2005). Within hours of particle exposure, alveolar macrophages have died by apoptosis or necrosis (Gilberti *et al.*, 2008; Joshi and Knecht, 2013). Because latex particles can be taken up as well and are completely nontoxic, there

This article was published online ahead of print in MBoC in Press (http://www.molbiolcell.org/cgi/doi/10.1091/mbc.E14-08-1301) on November 26, 2014.

*Present address: Center for Academic Programs, Unit 4170, University of Connecticut, 368 Fairfield Way, Storrs, CT 06269.

Address correspondence to: David A. Knecht (david.knecht@uconn.edu).

Abbreviations used: Ab, antibody; COZ, complement-opsonized zymosan; GFP, green fluorescent protein; PIP, phosphatidylinositol phosphate; PMA, phorbol myristate acetate.

is something about the chemistry of silica particles that is responsible for the surprisingly dramatic effect of such a ubiquitous and seemingly innocuous environmental material. After uptake, phagolysosomal membranes become compromised, leading to leakage of their contents into the cytoplasm (Thibodeau *et al.*, 2004). Many hours later, mitochondrial hyperpolarization, caspase-9 and -3 activation, nuclear changes, and eventually mitochondrial depolarization, phosphatidylserine exposure, and cell death occur in a temporal sequence (Shen *et al.*, 2001; Thibodeau *et al.*, 2003; Costantini *et al.*, 2011; Joshi and Knecht, 2013).

Of the known phagocytosis pathways, Fcγ receptor IIA (FcR)–mediated uptake has been studied in most detail. When an antibody (Ab)-opsonized particle comes in contact with a phagocyte, the Fc domain region of the antibody is bound by transmembrane surface receptors to trigger phagocytosis (Griffin *et al.*, 1976; Greenberg and Grinstein, 2002). Cross-linking of Fc receptors leads to activation by Src family tyrosine kinases Hck, Fgr, and Lyn (Ghazizadeh *et al.*, 1994), which phosphorylate the ITAM regions of the receptor (Daeron, 1997). The tandem SH2 domains of Syk bind to the ITAMs of the receptor, and Syk is activated by autophosphorylation (Kiefer *et al.*, 1998; Fitzer-Attas *et al.*, 2000). Phospholipase D then activates GTPase ARF6 to activate the Rho family small GTPases (Caumont *et al.*, 1998; Honda *et al.*, 1999; Caron, 2000). Cdc42 and Rac1 play a role in actin filament polymerization, which drives membrane around the particle, leading to phagosome formation (Cox *et al.*, 1997; Caron and Hall, 1998). Rho activation also occurs but may not be required for Fc receptor-mediated uptake (Hackam *et al.*, 1997; Caron and Hall, 1998).

Along with GTPase activation, a phosphatidylinositol lipid signaling cascade ensues to completely close the phagosome and subsequently traffic lysosomal vesicles to the phagosome (May, 2001). First, phosphatidyl-4-phosphate 5-kinase phosphorylates phosphatidylinositol (4)-phosphate to phosphatidylinositol (4,5)-bisphosphate (PI(4,5)P_2; Loijens *et al.*, 1996), which activates phosphoinositide 3 kinase-I (PI3 K-I) in order to phosphorylate PI(4,5)P_2 to phosphatidylinositol (3,4,5)-trisphosphate (PI(3,4,5)P_3; Marshall *et al.*, 2001; Greenberg and Grinstein, 2002; Vieira *et al.*, 2002; Gu *et al.*, 2003; Yeung *et al.*, 2006). At this stage, AKT can tether its PH domain to PI(3,4,5)P_3 (Marshall *et al.*, 2001). Subsequently, Arp2/3-dependent actin filaments assemble by zippering around the phagosome cup (Caron, 2000; May, 2000; Greenberg and Grinstein, 2002).

Once the phagosome is formed and internalized, the lipid composition of the membrane begins to undergo changes. This is also when depolymerization of actin filaments surrounding the phagosome occurs (Scott *et al.*, 2003, 2005; Yeung *et al.*, 2006). A PI(3,4,5)P_3 5′-lipid phosphatase, SHIP-I, dephosphorylates PI(3,4,5)P_3 to form phosphatidylinositol (3,4)-bisphosphate (Damen *et al.*, 1996). Subsequently, PI 3-kinase III (PI3 K-III) phosphorylates phosphatidylinositol (PI) to produce phosphatidylinositol (3)-phosphate (PI(3)P; Toker and Cantley, 1997). Phagosomes adopt early endosome markers (Rab5 GTPase and early endosome antigen-1) when endosomes fuse with phagosomes (Desjardins, 1995; Vieira *et al.*, 2001, 2003; Duclos *et al.*, 2003) and then lysosomal markers when lysosomes fuse with phagosomes to form a phagolysosome (Pitt *et al.*, 1992; Desjardins, 1995; Tjelle *et al.*, 2000; Vieira *et al.*, 2002; Duclos *et al.*, 2003). If the phagocytosed particle is a microorganism, acid hydrolases in the lysosome degrade the microorganism; however, there is no mechanism for lysosomal degradation of particles like silica and latex.

Complement receptor 3 (CR3)–mediated uptake of complement-opsonized particles such as complement-opsonized zymosan (COZ) shares some features with the FcR-mediated pathway, yet there are distinct mechanistic differences (Newman *et al.*, 1991; Allen and Aderem, 1996; Caron and Hall, 1998). Unlike FcR-mediated uptake, efficient complement-opsonized-particle uptake by CR3 (also known as integrin Cd11b/Cd18 or Mac-1) requires cells to be primed with phorbol 12-myristate 13-acetate (PMA) to activate protein kinase C signaling (Castagna *et al.*, 1982). Another mechanistic difference is the formation of an actin-rich cellular pedestal in the presence of complement-opsonized particles (Hall *et al.*, 2006; Bohdanowicz *et al.*, 2010; Lee *et al.*, 2011). The protrusion and uptake depend on the integrity of both the actin and microtubule cytoskeleton (Patel and Harrison, 2008). Phosphorylation of Src and Syk tyrosine kinases occurs during both types of uptake (Aderem and Underhill, 1999; Shi *et al.*, 2006), but RhoA GTPase is activated during CR3-mediated uptake rather than Rac GTPase. The phosphatidylinositol lipid signaling cascade that follows phagosome internalization (Bohdanowicz *et al.*, 2010) is similar for CR3- and FcR-mediated uptake (Bohdanowicz *et al.*, 2010).

In the present study, we compare the nonopsonized silica and latex particle uptake and processing pathway to the well-characterized FcR- and CR3-mediated pathways. GTPase and PI3K activation is similar to the opsonized-particle pathways except that nonopsonized particles activate both Rac and RhoA GTPases. Unlike FcR-mediated uptake, nonopsonized-particle uptake requires both actin and microtubule cytoskeletons. In addition, GTPase and PI3K activation requires the presence of microtubules. Finally, we establish that silica particles need to be internalized to be toxic, since binding of silica to the cell surface is insufficient to damage cells. Thus nonopsonized-particle uptake has unique characteristics that distinguish it from both FcR- and CR3-mediated uptake.

RESULTS

Pharmacological inhibitors of phagocytosis

To begin to characterize the nonopsonized-particle phagocytosis pathway, we treated cells with various pharmacological reagents that have been shown to inhibit FcR- and/or CR3-mediated uptake pathways. Phosphorylation of Fc-receptor ITAM regions by Src tyrosine kinases (Lyn, Hck, Fgr) and autophosphorylation of Syk tyrosine kinase are two of the initial steps of particle recognition during FcR-mediated phagocytosis (Kiefer *et al.*, 1998; Suzuki *et al.*, 2000). Inhibitors of tyrosine kinases reduce uptake through this pathway but have little effect on CR3-mediated uptake (Allen and Aderem, 1996). To address the requirement for tyrosine kinase activity for nonopsonized particles, we used PP2, a broad-spectrum tyrosine kinase inhibitor (Hanke *et al.*, 1996). Uptake of both Ab-opsonized and nonopsonized particles by macrophages treated with 20 µM PP2 was reduced by approximately 50% (Figure 1A and Supplemental Figure S1A), indicating a role for tyrosine kinases in both processes.

The next step of phagocytosis that is commonly observed is the activation of PI3 K-I, leading to the production of PI(3,4,5)P_3 (Cox *et al.*, 1999). Macrophages were treated with either 20 nM wortmannin or 20 µM LY294002 to inhibit PI3 K-I and then exposed to particles. Uptake of both Ab-opsonized and nonopsonized particles was significantly reduced in the presence of either compound (Figure 1B and Supplemental Figure S1B). These data suggest that PI3 K-I activation plays a similar role during both FcR-mediated and nonopsonized-particle phagocytosis.

Cytoskeletal actin filaments are polymerized to protrude the membrane and surround the particle during internalization by macrophages (Swanson, 1995; Machesky, 1999; May, 2000). To determine the role of actin filament polymerization during

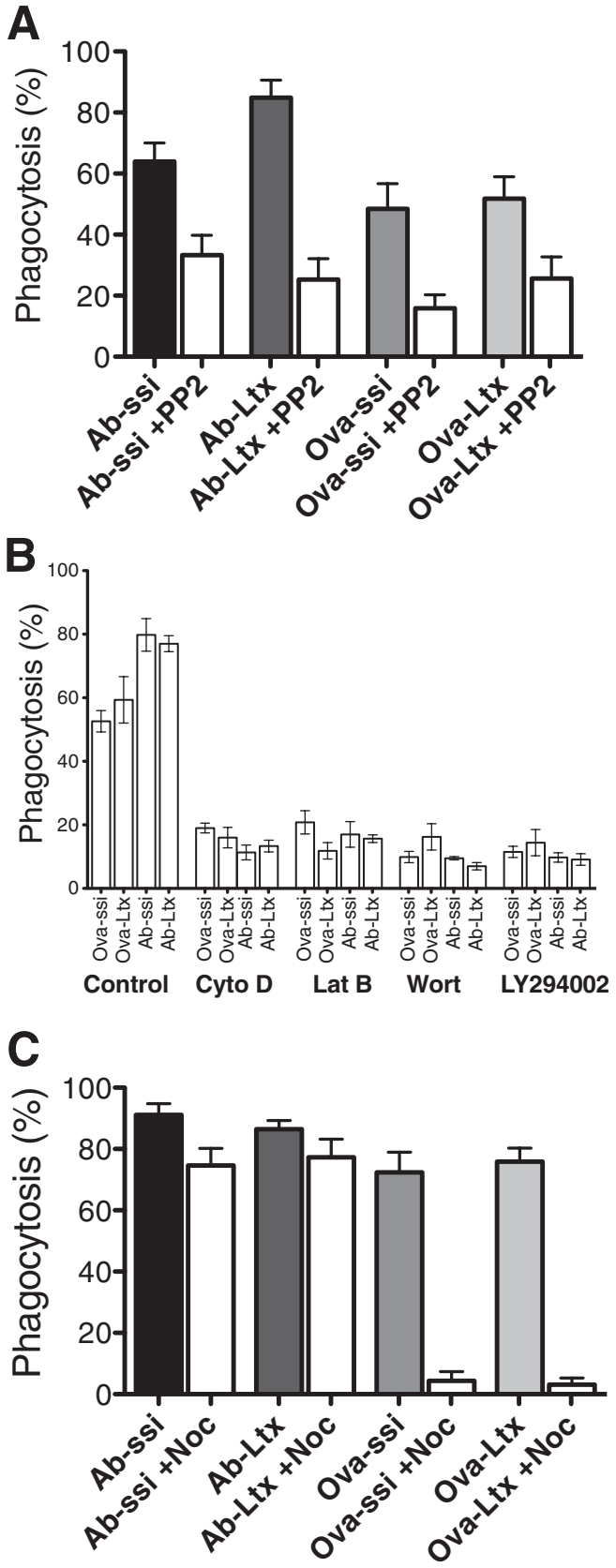

FIGURE 1: The effect of pharmacological inhibitors on particle uptake. Cells were treated with inhibitors for (A) tyrosine phosphorylation (20 μM PP2), (B) PI3 K-I (20 μM LY294002, 20 nM wortmannin [Wort]), or actin polymerization (500 nM latrunculin B [Lat-B], 500 nM cytochalasin D [Cyto-D]), or (C) microtubule polymerization (800 nM nocodazole [Noc]) and subsequently exposed to Ab-opsonized spherical silica or latex (Ab-ssi, Ab-Ltx) or nonopsonized spherical silica or latex (Ova-ssi, Ova-Ltx) particles for 45 min. The presence of inhibitor in A and B results in a decreased amount of both Ab-opsonized- and nonopsonized-particle uptake, but only nonopsonized-particle uptake in C is affected by the presence of nocodazole. Error bars represent SEM of at least three experiments performed in duplicate on separate days.

nonopsonized-particle uptake, we tested inhibitors of cytoskeletal filament formation. Cells were treated with either 500 nM latrunculin B or 500 nM cytochalasin D to inhibit actin polymerization before particle addition. Both drugs dramatically inhibited uptake of particles (Figure 1B and Supplemental Figure S1B), consistent with the observation of an actin-rich phagosome surrounding nonopsonized silica particles (Haberzettl *et al.*, 2007; Costantini *et al.*, 2011).

CR3-mediated uptake of complement-opsonized particles, but not FcR-mediated uptake of Ab-opsonized particles, depends on an intact microtubule cytoskeleton (Newman *et al.*, 1991; Allen and Aderem, 1996). To determine whether nonopsonized-particle uptake requires microtubules, we treated cells with nocodazole before particle exposure. To minimize potential off-target effects of the compound, the minimum concentration of nocodazole necessary to depolymerize microtubules, 800 nM, was used (Supplemental Figure S2). Consistent with earlier results, Ab-opsonized-particle uptake was unaffected by nocodazole treatment (Figure 1C and Supplemental Figure S1C; Newman *et al.*, 1991; Allen and Aderem, 1996). Surprisingly, nocodazole not only inhibited CR3-mediated uptake, but it also blocked internalization of both nonopsonized silica particles and latex beads (Figure 1C and Supplemental Figure S1C). This result indicates that nonopsonized-particle uptake is distinct from FcR-mediated uptake. It is also distinct from CR3-mediated uptake because in order for cells to take up complement-opsonized particles, they must be preactivated with PMA (Castagna *et al.*, 1982; Allen and Aderem, 1996). Uptake of nonopsonized particles does not require PMA activation. Of interest, the fact that untreated cells cannot take up complement-opsonized COZ indicates that not all types of particles encountered by cells can be taken up by the nonopsonized uptake pathway.

Rho-family GTPases are activated during nonopsonized-particle uptake in a microtubule-dependent manner

FcR engagement with Ab-opsonized particles triggers activation of Rac1 GTPase and Cdc42, whereas binding of complement-opsonized particles to CR3 triggers activation of RhoA GTPase (Caron and Hall, 1998; Caron, 2000; Caumont *et al.*, 1998; Honda *et al.*, 1999). To establish which Rho-family GTPases are activated in the presence of nonopsonized particles, we exposed cells to nonopsonized particles, Ab-opsonized particles, or COZ and measured the extent of GTPase activation. Within 30 s, COZ and nonopsonized particles activated RhoA to a similar extent and with similar timing (Figure 2A), whereas Ab-opsonized particles showed little activation. Cells exposed to Ab-opsonized particles activated Rac within 30 s (Figure 2B), whereas it took 15 min to see a comparable activation of Rac with nonopsonized particles (Figure 2B). There was no significant activation of Rac by COZ. Thus, unlike FcR- and CR3-mediated phagocytosis, both Rac and RhoA GTPases are activated during nonopsonized-particle uptake.

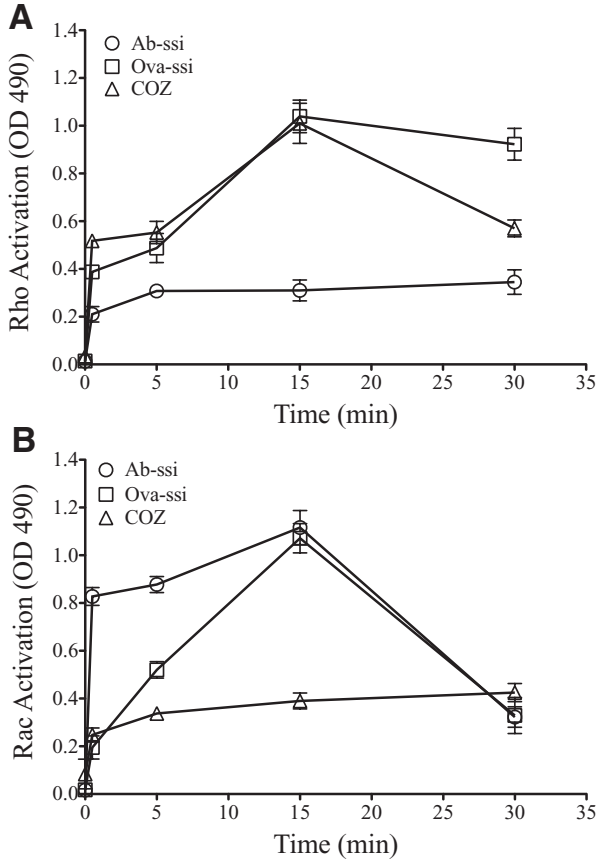

FIGURE 2: Exposure to nonopsonized particles activates RhoA and Rac GTPase. Macrophages were exposed to antibody-opsonized spherical silica (Ab-ssi; circles), ovalbumin-coated spherical silica (Ova-ssi; squares), or COZ (triangles) for increasing time points before lysate collection. The kinetics of activation of either RhoA GTPase (A) or Rac GTPase (B) was measured by HRP absorbance at 490 nm using a G-LISA fluorescence detection assay. The kinetics is slower than during other assays due to acclimation to a synchronization temperature. Maximum activation of both Rac and RhoA occurs by 15 min after exposure. Only nonopsonized particles elicit both RhoA and Rac GTPase activation. Error bars represent SEM of two experiments performed in duplicate on two separate days.

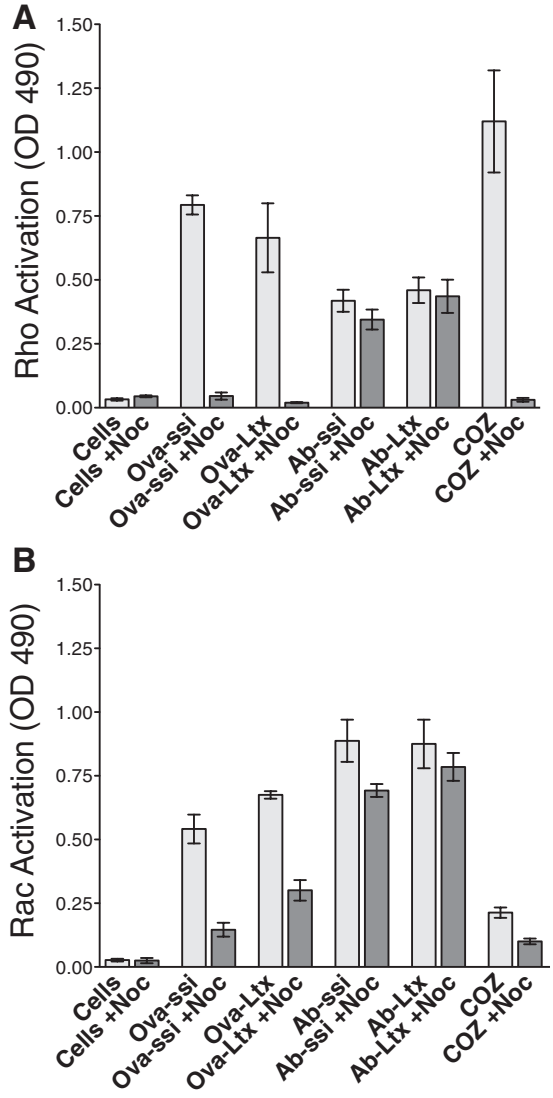

FIGURE 3: Neither RhoA nor Rac is activated upon nonopsonized particle exposure in the presence of nocodazole. Cells were treated with 800 nM nocodazole (Noc) and subsequently exposed to no particles (Cells), nonopsonized particles (Ova-ssi, Ova-Ltx), antibody-opsonized particles (Ab-ssi, Ab-Ltx), or COZ for 15 min. Activation of RhoA (A) or Rac (B) GTPase was measured by HRP absorbance at 490 nm using a G-LISA fluorescence detection assay. In the presence of Noc (dark gray bars), RhoA and Rac GTPase activation are diminished when cells are exposed to Ova-ssi, Ova-Ltx, or COZ but not Ab-ssi or Ab-Ltx. Error bars represent SEM of two experiments performed in duplicate on two separate days.

Because nocodazole inhibited the uptake of nonopsonized particles, it was important to determine the stage at which this inhibition occurs. To establish whether microtubules are required before GTPase activation, we treated cells with nocodazole and then exposed them to particles for 15 min. Nocodazole inhibited RhoA and Rac activation in cells exposed to nonopsonized particles (Figure 3, A and B) and inhibited RhoA activation in cells exposed to COZ particles (Figure 3A). As expected, the depolymerization of microtubules did not affect the activation of Rac in cells exposed to Ab-opsonized particles (Figure 3B). Thus microtubules seem to be involved at an early step in the process of phagocytosis of COZ and nonopsonized particles.

Silica is cytotoxic to macrophages and activates both Rac and RhoA GTPase. It is possible that activation of both GTPases is an important part of the pathway that leads to silica-induced cell death. To test this hypothesis, we exposed cells to nonopsonized or Ab-opsonized 3-μm latex beads, which are not toxic to cells, and measured the activation of GTPases. The results were similar to those obtained with silica particles. Nonopsonized latex beads activated both RhoA and Rac GTPases, whereas Ab-opsonized latex beads showed greater Rac activation. In the presence of nocodazole, the GTPases were not activated by nonopsonized particles but were activated by Ab-opsonized particles (Figure 3, A and B). Therefore simultaneous activation of both Rac and RhoA is not sufficient to cause cell death. In addition, the data show that the dual GTPase activation is not related to some specific characteristic of silica particle surface chemistry.

PI(3,4,5)P_3 accumulation on nonopsonized particle phagosomes is a microtubule-dependent process

The data in Figure 1 indicate that PI3 K-I activation is required for Ab-opsonized- and nonopsonized-particle uptake. To determine whether the spatial and temporal dynamics of PI(3,4,5)P_3

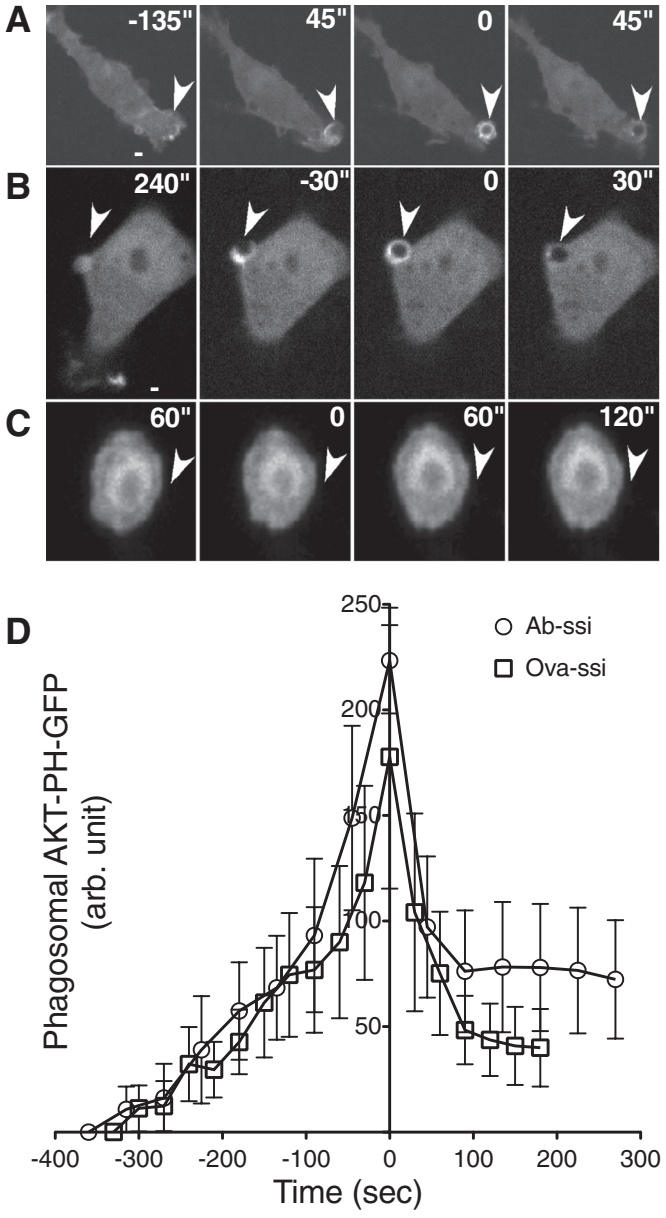

FIGURE 4: PI(3,4,5)P3 concentrates at nonopsonized-particle phagosomes but not in the presence of nocodazole. Cells were transiently transfected with AKT-PH-GFP to detect accumulation of PI(3,4,5)P3 at particle phagosomes. When exposed to (A) Ab-opsonized spherical silica or (B) ovalbumin-coated spherical silica, AKT-PH-GFP quickly concentrates at the site of the particle and dissociates once a particle has been internalized. (C) When cells are treated with 800 nM nocodazole, AKT-PH-GFP does not accumulate around nonopsonized- particle phagosomes. These data are representative of localization visualized on six separate days. (D) The rate of AKT-PH-GFP association with and dissociation from particle phagosomes. $N = 12$. Time zero represents maximum localization after particle–cell interaction, and error bars represent SEM.

accumulation at sites of phagocytosis differ between Ab-opsonized and nonopsonized particles, we imaged cells expressing AKT-PH–green fluorescent protein (GFP) during phagocytosis. When these cells were exposed to Ab-opsonized or nonopsonized particles, AKT-PH-GFP rapidly accumulated around both types of nascent phagosomes (Figure 4, A and B). Before particles were completely internalized, the probe dissociated from the phagosome. The extent of accumulation and the time course of association and dissociation were similar for Ab-opsonized and nonopsonized silica particles (Figure 4D), as well as 3-μm (Ab-opsonized and nonopsonized) latex beads (unpublished data), suggesting that all particle types activate PI3 K-I equivalently. When cells were treated with either wortmannin or LY294002 before particle addition, no nascent phagosomes were formed, and AKT-PH-GFP did not accumulate at sites where particles were bound to the cell (unpublished data). To test whether microtubules are required for PI3K activation, we treated macrophages transiently expressing AKT-PH-GFP with nocodazole and then exposed them to silica particles. AKT-PH-GFP accumulated at Ab-opsonized-particle phagosomes (unpublished data) but did not accumulate at sites where nonopsonized particles were bound to cells (Figure 4C), suggesting that PI3 K-I activation also depends on the presence of microtubules during nonopsonized-particle uptake.

Actin polymerization during particle phagocytosis is a microtubule-dependent process

The kinetics of F-actin accumulation around Ab-opsonized particles during Fc receptor–mediated phagocytosis is well characterized (Swanson, 1995; Machesky, 1999; May, 2000). To study F-actin dynamics during nonopsonized-particle phagocytosis, we exposed macrophages stably expressing GFP-actin to nonopsonized or Ab-opsonized particles. Actin accumulates around both particle types at a similar rate and to a similar extent during uptake (Figure 5, A, B, and E). Once particles are internalized, actin dissociates from both types of phagosomes at a similar rate. Actin-rich pseudopods also accumulate around COZ particles, but only when cells were stimulated with PMA before particle addition (Supplemental Figure S3). Without PMA treatment, no actin response was observed, and there was no uptake of particles. Further, when PMA-treated cells were exposed to zymosan that was not complement opsonized, there was no actin localization and no uptake (unpublished data).

We have established that the microtubule network is necessary for RhoA and Rac GTPase activation, as well as for PI3 K-I activation. To determine whether the presence of microtubules also affects actin accumulation at sites of phagocytosis, we treated cells expressing GFP-actin with nocodazole and then exposed them to nonopsonized or Ab-opsonized silica or COZ. F-actin localized around Ab-opsonized particles with kinetics similar to untreated cells (Figure 5, C and F, and Supplemental Video S1). No localization of the actin probe was observed at sites where nonopsonized particles (Figure 5D and Supplemental Video S2) or COZ particles were bound to cells (unpublished data).

We noticed that when cells were treated with nocodazole, the GFP-actin probe rapidly accumulated in the peripheral cell cortex (Figure 5, C and D, and Supplemental Figure S4, A and C). When cells were treated with nocodazole and subsequently fixed and stained with rhodamine phalloidin, there was an increase in the total cortical F-actin as well (Supplemental Figure S4, B and D). This result indicates that there is a general change in the structure of the cortical cytoskeleton in response to microtubule depolymerization. This change may provide a clue as to why cells without intact microtubules are unable to phagocytose some types of particles.

To better understand whether F-actin polymerization contributes to Ab-opsonized- and nonopsonized-particle phagosome initiation and maturation to a similar extent, we treated stably transfected GFP-actin macrophages with either cytochalasin D or latrunculin to

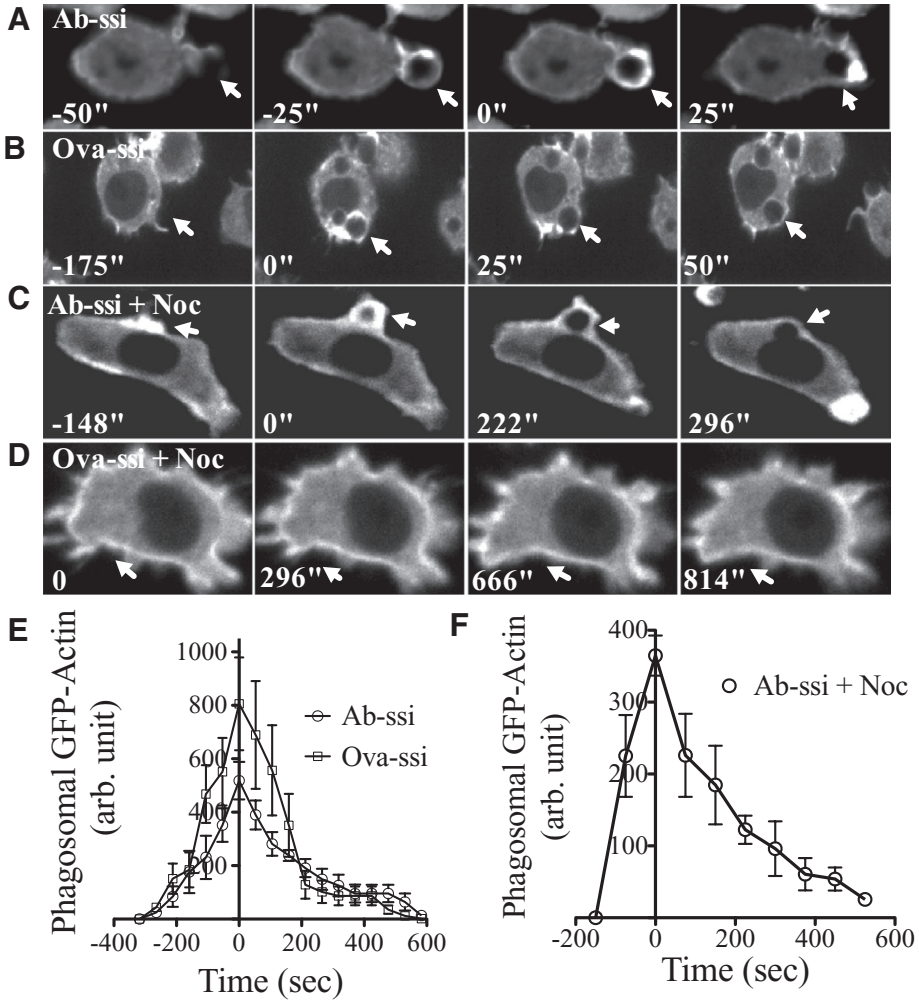

FIGURE 5: Actin-rich protrusions do not extend around nonopsonized-particle phagosomes when microtubules are depolymerized. GFP-actin macrophages were exposed to either (A) Ab-opsonized or (B) nonopsonized particles and imaged to determine the time course of actin ring association with particle phagosomes. Actin-rich phagosomes form around, and dissociate from, Ab-opsonized and nonopsonized particles on a similar time scale. When cells were treated with 800 nM nocodazole, actin associated with Ab-opsonized-particle phagosomes (C) but not nonopsonized-particle phagosomes (D). (E, F) The time course of actin association with and dissociation from particle phagosomes is similar when cells are exposed to either Ab-opsonized or nonopsonized particles. $N = 40$. Time zero represents maximum localization after particle–cell interaction. (F) The time course of actin association with and dissociation from Ab-opsonized particle phagosomes in the presence of nocodazole. Time zero represents maximum localization after particle–cell interaction. $N = 4$. Error bars represent SEM.

inhibit actin polymerization and then exposed them to either Ab-opsonized or nonopsonized silica. In the presence of cytochalasin D, both particle types formed punctate actin spots (Supplemental Figure S5A). In the presence of latrunculin, cells exposed to Ab-opsonized silica formed a punctate spot at the site of particle binding, but the cup never surrounded the particle, whereas cells exposed to nonopsonized silica did not show any actin response at all (Supplemental Figure S5B).

Because microtubules are necessary for nonopsonized-particle uptake, it is possible that surface-bound particles might be internalized after repolymerization of microtubules. Nonopsonized particles were allowed to bind to cells in the presence of nocodazole for 45 min, and then microtubules were allowed to repolymerize by changing the cells to fresh medium without nocodazole. Within 5 min of nocodazole washout, microtubules had repolymerized (unpublished data). Nonopsonized silica particles that were attached to the cells were not internalized over the next 2 h (Supplemental Figure S6, arrowhead). However, nonopsonized latex particles added to the cells after nocodazole was removed were internalized within 10 min (Supplemental Figure S6, arrow). The same phenomenon was observed when the order of addition of the particles was reversed (unpublished data). These data indicate that the presence of microtubules is not sufficient to drive phagocytosis of nonopsonized particles, but instead that a dependent sequence of events appears to be required.

Endolysosomal vesicle fusion with phagosomal membranes occurs once actin dissociates from particle phagosomes

As FcR-mediated phagosome maturation progresses, membrane is contributed to the nascent phagosome from endosomal and lysosomal vesicles (denoted as endolysosomal vesicles) fusing with phagosomes (Bajno *et al.*, 2000). GFP-actin–expressing macrophages were incubated with red fluorescent dextran for 90 min to label endolysosomal compartments and then exposed to silica particles. The phagosomes gradually increased in fluorescence intensity after the particles were internalized (Figure 6A and Supplemental Video S3). The actin associated with phagosomes disappears before detection of an increase in dextran fluorescence, indicating that it is the internalized, actin-free phagosome to which the endolysosomal vesicles fuse. The time course and extent of increase in fluorescence intensity due to endolysosomal vesicle fusion were similar for Ab-opsonized and nonopsonized silica particles (Figure 6B).

Appearance of PI(3)P around nonopsonized particle phagosomes

After endosomes fuse with phagosomes, PI(3)P can be detected in association with the phagosomal membrane (Vieira *et al.*, 2001). To determine whether the vesicle trafficking pathway reaches this step during nonopsonized-particle phagosome maturation, we exposed macrophages transiently expressing 2xFYVE-GFP, a probe for PI(3)P, to either Ab-opsonized or nonopsonized spherical silica particles. The probe was recruited similarly to the membranes surrounding both particle types (Figure 7), suggesting that both undergo the same vesicle trafficking events once taken up into cells. Cells transiently cotransfected with Ruby-Lifeact and 2xFYVE-GFP show that actin associates with both Ab-opsonized- and nonopsonized-particle phagosomes before 2xFYVE-GFP associates with the phagosome (Supplemental Video S4). Sometimes the Lifeact signal is completely lost from phagosomes before 2xFYVE-GFP appears, and sometimes the two signals overlap. These results indicate that the later events in vesicle trafficking are similar for opsonized and nonopsonized phagosomes.

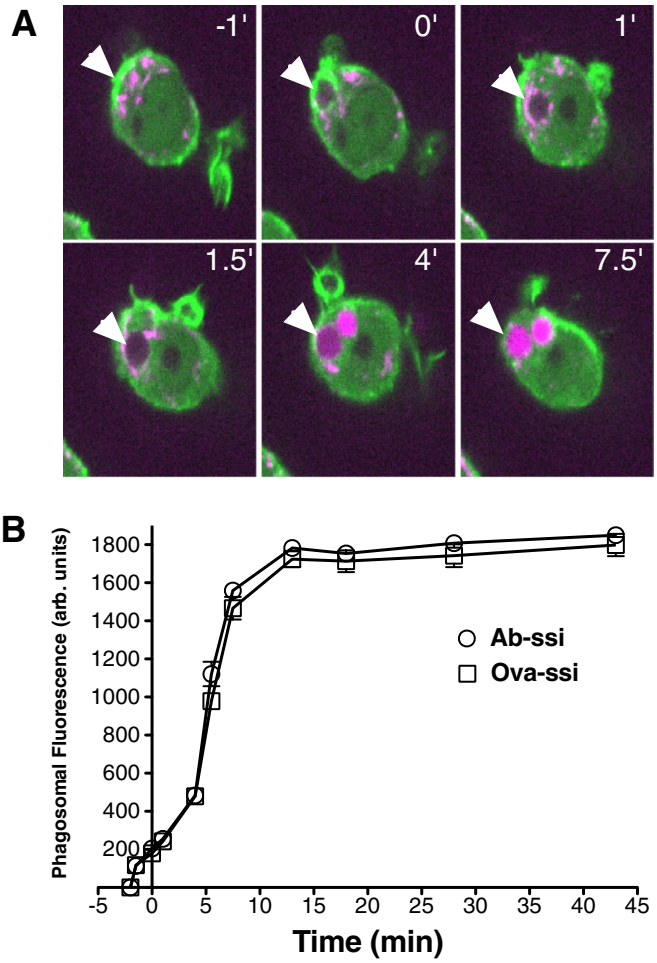

FIGURE 6: Actin dissociation precedes endolysosomal vesicle fusion with phagosomal membranes. (A) GFP-actin macrophages were preloaded with a red fluorescent dextran before particle addition. Actin rings (green) formed around nonopsonized particles (arrowheads) and then dissociated rapidly after internalization. Phagosomes then increased in red fluorescence intensity due to endolysosome fusion (shown in magenta). (B) Quantification of phagosomal dextran fluorescence for opsonized and nonopsonized silica particles. $N = 30$. Time zero represents the time when the actin ring first begins to form. Error bars represent SEM.

PI3 kinase-I activation, actin polymerization, and microtubule polymerization are necessary for silica-induced cell death in macrophages

Because cells bind but do not internalize particles in the presence of several pharmacological inhibitors, we were able to address the question of whether silica toxicity requires particle internalization or, alternatively, whether particle surface binding is sufficient to induce cell death. In the absence of inhibitors, 50–100% of the cells die within 10 h when macrophages are exposed to nonopsonized silica particles (Gilberti *et al.*, 2008). Cells were treated with silica particles plus concentrations of wortmannin, LY294002, cytochalasin D, latrunculin, or nocodazole that inhibit phagocytosis but are not toxic to cells (Supplemental Figure S7). The inhibitor-treated cells had an equivalent number of surface-bound particles as the untreated cells normally internalize (unpublished data); however, the surface-bound particles were not toxic (Figure 8). These data suggest that particle internalization is necessary to induce cell death.

DISCUSSION

When a particle interacts with a cell surface, a transmembrane receptor typically recognizes the particle and initiates phagocytosis. For Ab- and complement-opsonized particles, the receptors and their interaction with particles have been extensively studied. However, whether there is a specific cell-surface molecule that interacts with nonopsonized particles is unclear. There is evidence that scavenger receptor family-A receptors (SR-A) may play a role in recognizing negatively charged silica particles (Taylor *et al.*, 2005); however, uptake of silica also occurs in SR-A–deficient cells (Hamilton *et al.*, 2006; Thakur *et al.*, 2009), and there is no reason to expect SR-A to interact with latex particles, which are also readily internalized. More important, we found no difference in the uptake of silica coated with proteins of various charge or of latex beads that have negative, positive, or neutral surface charges (Gilberti *et al.*, 2008). Furthermore, uptake occurs similarly whether particles are uncoated or ovalbumin coated (Costantini *et al.*, 2011). There is no reason to suspect that cells have evolved specific uptake machinery for a particle surface that macrophages rarely encounter. We hypothesize that nonopsonized particles are internalized by a nonspecific mechanism involving surface charge interaction. There are sufficient mobile charged molecules in the plasma membrane for us to presume that local charges can rearrange to allow for a stable particle–cell interaction.

Once particles are bound, cells seem to nonspecifically activate the phagocytosis machinery. This normally occurs due to receptor clustering, but it appears that nonspecific binding can activate normal phagocytosis. In our model, receptor clustering at the site of nonspecific binding triggers phagocytosis. This is consistent with the fact that FcR expression in FcR-deficient COS-7 cells allows for efficient phagocytosis of Ab-opsonized particles in a manner similar to macrophages, which normally express FcR (Indik *et al.*, 1991). There are notable differences in the uptake machinery of FcR- and CR3-mediated uptake. FcR-mediated uptake is independent of macrophage activation and the presence of microtubules (Newman *et al.*, 1991; Allen and Aderem, 1996). CR3-mediated uptake requires activation of macrophages by PMA (Castagna *et al.*, 1982) and is dependent on microtubules (Newman *et al.*, 1991; Allen and Aderem, 1996). We have now established the events that occur in nonspecific particle phagocytosis once binding occurs, regardless of the mechanism of binding.

To investigate the molecular pathway of nonopsonized-particle phagocytosis, a variety of markers were chosen that have been well characterized for FcR- and CR3-mediated uptake. We considered the possibility that some difference in the uptake and vesicle trafficking pathway for nonopsonized particles might play an important role in silica particle toxicity. Our results show that, for the most part, the opsonized and nonopsonized pathways share many properties. More important, nonopsonized silica (toxic) and nonopsonized latex (nontoxic) were indistinguishable with the probes we examined. There are interesting differences between nonopsonized- and opsonized-particle uptake. Nonopsonized particles activate both RhoA and Rac GTPase, whereas only Rac is activated during FcR-mediated uptake, and only RhoA is activated during CR3-mediated uptake (Figure 2). Although it is possible that dual GTPase activation might relate to the toxicity of nonopsonized silica, this seems unlikely since similar results were obtained upon exposure to nonopsonized, nontoxic latex beads, suggesting that this is a characteristic of nonopsonized-particle uptake. Thus it does not appear that silica toxicity is related to a particular pathway associated with nonopsonized-particle uptake.

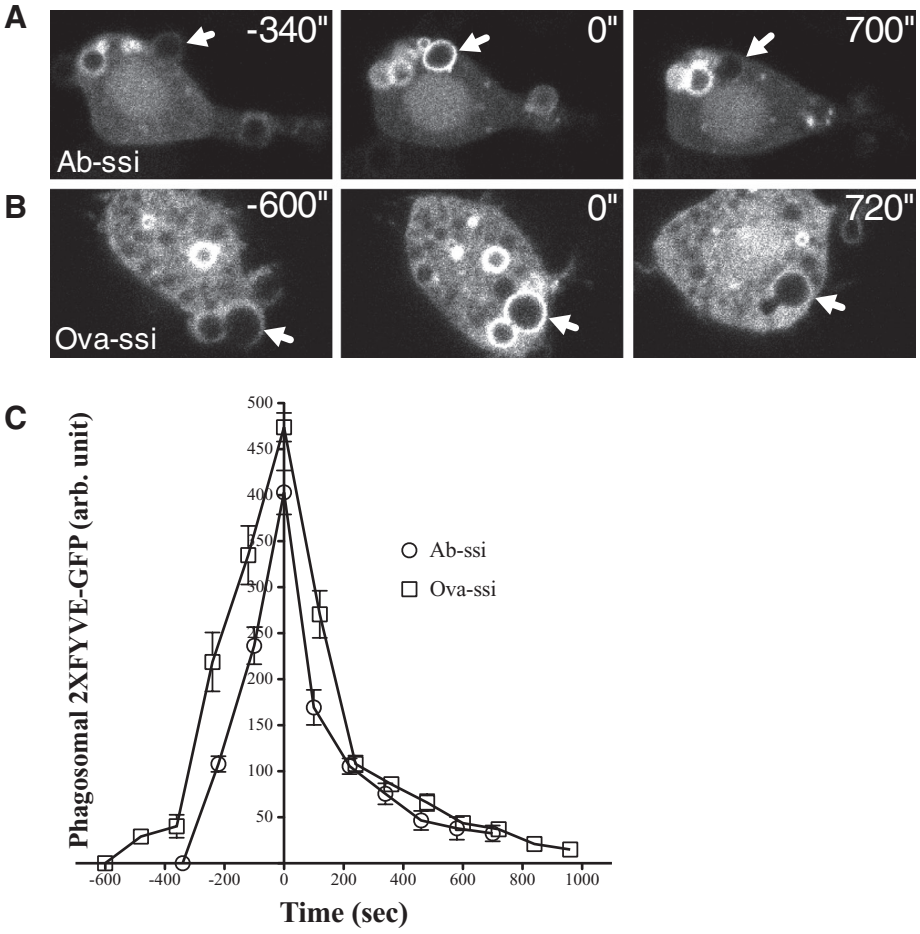

FIGURE 7: PI(3)P tethers to nonopsonized-particle phagosomes. Cells were transiently transfected with vector expressing 2xFYVE-GFP to detect accumulation of PI(3)P. When cells were exposed to (A) Ab-opsonized or (B) nonopsonized spherical silica, 2xFYVE-GFP accumulates at phagosomes within 6 min relative to initial particle–cell interaction and persists long after the particle has been internalized. (C) Quantification of the association of 2xFYVE-GFP with phagosomes. $N = 6$. Time zero indicates maximum accumulation of 2xFYVE-GFP at particle phagosomes. 2xFYVE-GFP accumulates at and dissociates from opsonized and nonopsonized particle phagosomes at a similar rate. Error bars represent SEM.

The most important difference in the uptake pathway of nonopsonized particles is that, like complement-opsonized particles, nonopsonized-particle uptake depends on microtubules. Depolymerization of microtubules blocks particle uptake and toxicity (Figures 1 and 8 and Supplemental Figure S2). However, whereas CR3-mediated uptake requires macrophages to be primed with PMA, nonopsonized phagocytosis does not require preactivation. Of interest, non–complement-opsonized yeast or zymosan particles are not internalized even if cells are initially primed. These data suggest that not all particle types that cells encounter are susceptible to nonspecific, nonopsonized-particle phagocytosis. Whether it is the microtubules themselves or something associated with the microtubule that is required for phagocytosis remains unclear. We have been unable to image individual microtubules in macrophage cell lines, so we cannot say whether there is an altered accumulation of microtubules at sites of phagocytosis. Evidence indicates that CLIP-170 plays an important role in CR3-mediated phagocytosis through its interaction with mDia (Lewkowicz *et al*., 2008), so it is likely that a similar interplay of microtubules, microtubule-associated proteins, and actin nucleation factors is required for nonopsonized-particle phagocytosis.

In the presence of nocodazole, nonopsonized particles do not stimulate a significant Rac or RhoA GTPase response (Figure 3), and there is no PI(3,4,5)P_3 or F-actin localization at the site of particle–cell interaction (Figures 4 and 5). Thus microtubules are needed to initiate the phagocytosis machinery from the earliest known part of the pathway. To further elucidate the role of microtubules during uptake, we treated GFP-actin–expressing macrophages with nocodazole, exposed them to nonopsonized particles that bound to the cells, and then removed nocodazole from the culture media to allow microtubules to regrow. When the cells were then exposed to new, nonopsonized particles, only the particles that were added after removing nocodazole were internalized (Supplemental Figure S6). The particles initially added to the cells were still bound to the cells but never internalized. These data suggest that when a particle binds to a cell, a signal transduction cascade is initiated that requires microtubules. The initial activation event then likely becomes attenuated so that even when microtubules are repolymerized, the activation signal is not sent, and the particles are never taken up.

Another interesting effect of nocodazole treatment is a change in overall F-actin distribution in cells (Supplemental Figure S4). Rapid accumulation of F-actin around the cell periphery occurs when microtubules are depolymerized. This result is consistent with evidence for interaction between the microtubule and actin cytoskeletons (Bartolini and Gundersen, 2010; Zhou *et al*., 2010a,b; Dent *et al*., 2011). In the absence of microtubules, cells may lose control of specific sites of actin polymerization and/or depolymerization, leading to wholesale accumulation of F-actin around the periphery of the cell. Thus it is possible that the lack of uptake may be due to an overabundance of F-actin in the cytoskeleton rather than an inability to polymerize actin at a specific site. However, it should be noted that Ab-opsonized particles are still taken up under these conditions.

Even though these studies have provided insight into how nonopsonized particles are internalized, they do not directly inform us about a crucial aspect of the process—how silica particles induce cell death. Leakage from phagolysosomal compartments is the earliest known event in silica-induced cell death (Thibodeau *et al*., 2004; Costantini *et al*., 2011; Joshi and Knecht, 2013). Leakage occurs within 90 min after particle exposure, and cell death occurs many hours later. Our initial hypothesis was that some aspect of signaling or vesicle processing might be altered in silica phagocytosis, and this might make phagosomes particularly sensitive to reactive oxygen or other factors that could lead to lysosomal membrane damage (Thibodeau *et al*., 2004; Costantini *et al*., 2011; Joshi and Knecht, 2013). However, leakage occurs with nonopsonized silica but not latex particles (unpublished data), even though both appear to be taken up by the same pathway. Our results suggest that

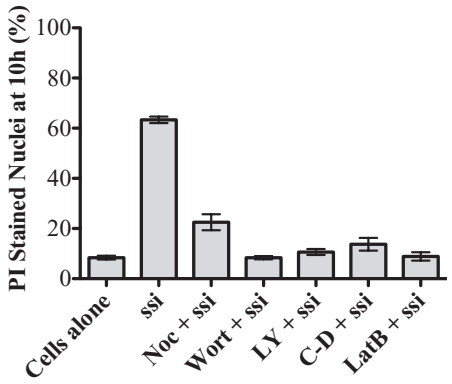

FIGURE 8: Phagocytosis is necessary to trigger silica-induced cell death in macrophages. Cells were treated with nocodazole (Noc), cytochalasin D (C-D), latrunculin B (LatB), LY294002 (LY), or wortmannin (wort), at the concentrations used to inhibit phagocytosis, in the presence of propidium iodide to measure the extent of membrane-permeable cells at 10 h. Nonopsonized, ovalbumin-coated 3 μm spherical silica (ssi) particles are only toxic to cells in the absence of inhibitor. Error bars represent SEM.

nonopsonized uptake of silica and latex are equivalent, indicating that the difference in toxicity is due to some aspect of the chemistry of the silica particle itself. This is consistent with measurements of increased reactive oxygen species (ROS) in cells treated with silica particles (Blackford *et al.*, 1994; Vallyathan and Shi, 1997; Fubini, 1998; Huaux, 2007). Our observation that silica particles need to be internalized to be toxic (Figure 8) supports the hypothesis that if ROS is the culprit, the focus should be on phagosomal ROS formed during the respiratory burst associated with macrophage phagocytosis.

MATERIALS AND METHODS

Chemicals

All chemicals are from Sigma Chemical (St. Louis, MO), unless otherwise noted.

Tissue culture

The mouse alveolar macrophage cell line MH-S (ATCC CRL-2019) was cultured at 37°C with 5% CO_2 in RPMI-1640 medium (Media Tech, Pittsburgh, PA) supplemented with 2 mM L-glutamine, 1 mM sodium pyruvate, 10 mM 4-(2-hydroxyethyl)-1-piperazineethanesulfonic acid, 55 μM 2-mercaptoethanol, 10% fetal bovine serum (FBS; Atlanta Biologicals, Lawrenceville, GA), 100 μg/ml ampicillin, and 100 μg/ml dihydrostreptomycin sulfate.

Particles

The particles used were amorphous 3-μm spherical silica (Allsphere silica; Alltech Associates, Deerfield, IL), zymosan A (Sigma Chemical), and 3-μm plain latex beads (Polysciences, Warrington, PA). Ovalbumin-coated (nonopsonized) particles were made by incubating 2 mg of spherical silica or 100 μl of latex beads in 1 ml of 10 mg/ml ovalbumin in particle-coating buffer (1.8 mM Na_2CO_3, 3.2 mM $NaHCO_3$, 135 mM NaCl, pH 9.5) for 90 min at 37°C while tumbling. Ab-opsonized silica and latex beads were made by incubating the ovalbumin-coated particles with 20 μg/ml rabbit anti–chicken egg albumin (Immunology Consultants Laboratory, Newberg, OR) in 1 ml of phosphate-buffered saline (PBS) for 90 min at 37°C while tumbling. COZ particles were made by incubating 2 mg of zymosan A with 1 ml of non–heat-inactivated FBS for 90 min at 37°C while tumbling. All particles were stored at 4°C for a maximum of 1 mo and centrifuged and washed three times in 1× sterile PBS before addition to cells.

Transfection of MH-S macrophage cells

MH-S macrophages were plated in a 35-mm WillCo (WillCo Wells, Amsterdam, Netherlands) or ibidi (ibidi, Munich, Germany) dishes in 1 ml of RPMI-1640 complete medium at 37°C with 5% CO_2 and allowed to adhere overnight. The next day, cells were transiently transfected with FuGeneHD transfection reagent (Promega, Madison, WI) and 2 μg of DNA in complete medium according to manufacturer's guidelines and allowed to incubate at 37°C overnight. Fluorescent cells were used within 24–48 h. Cells were also transiently cotransfected with Ruby-Lifeact (Riedl *et al.*, 2008) and either AKT-PH domain fused to enhanced GFP (AKT-PH-GFP; Varnai and Balla, 1998) or 2xFYVE domain fused to green fluorescent protein (2xFYVE-GFP; Vieira *et al.*, 2001). To examine actin dynamics during phagocytosis, cells were transfected by electroporation with a pEF6-GFP-actin probe, and a stably expressing clone was picked after selection of transformants with 3 μg/ml blasticidin (Scott *et al.*, 2005). To maintain the stable cell line, fluorescent colonies were manually picked after limiting dilution cloning.

Time-lapse confocal microscopy

Stable GFP-actin MH-S macrophages expressing fluorescent reporter probes were plated at 1×10^5 cells/cm^2 in ibidi or WillCo dishes in 1 ml of RPMI-1640 complete medium and allowed to adhere overnight. Medium was then replaced with 1 ml of CO_2-independent medium (Invitrogen, Carlsbad, CA), and cells were maintained at 37°C in an ambient atmosphere incubator for 15 min before being moved to the microscope stage, where they were maintained at 37°C in a LiveCell chamber (Pathology Devices, Westminster, MD). If cells were to be transiently transfected, they were plated at a lower density so that they would be at the same density of 1×10^5 cells/cm^2 for the microscopy assay. The same dish was used for transfection and subsequent imaging. Cells were transiently transfected in an ibidi or WillCo dish following the same protocol as before and remained in the dish in complete medium overnight. Medium was replaced with 1 ml of CO_2-independent medium, and cells were maintained at 37°C in an ambient atmosphere incubator for 15 min before being moved to the microscope stage, where they were maintained at 37°C in a LiveCell chamber.

Cells that would be exposed to COZ were treated with 100 nM PMA in CO_2-independent medium for 30 min at 37°C in an ambient atmosphere incubator. Time-lapse imaging was initiated, and then 15 μg/cm^2 silica, 40-μl latex beads, or 8 μg/cm^2 COZ was added to the cells. All three concentrations yield about 5 particles/cell. This concentration of silica is toxic to macrophages but also provides a low number of particles per cell to analyze phagocytosic processes.

Using a motorized *XYZ* stage, multiple fields of view and multiple *Z*-planes were captured over time. Differential interference contrast (DIC) and confocal fluorescence images were acquired using a Clara Interline charge-coupled device camera on an Andor spinning disk confocal microscope (Andor Technology, Belfast, Northern Ireland) or a Nikon A1R laser scanning confocal microscope (Nikon, Melville, NY). Particles were not all internalized in a single plane, so the most representative slice was chosen from the stack for each particle. Images were processed using ImageJ (National Institutes of Health, Bethesda, MD) to measure the increase and decrease in probe localization during uptake. Image stacks were also converted to QuickTime movies (Apple, Cupertino, CA) to observe time-lapse fluorescent protein localization and particle internalization. To

measure the timing of actin, $PI(3,4,5)P_3$, and PI(3)P association with and subsequent dissociation from particle phagosomes, a circle was drawn around the circumference of the particle at the initial location of particle–cell interaction. Mean fluorescence intensity was determined as the GFP probe associated with and subsequently dissociated from the particle phagosome over time. Time zero represents the maximum intensity of fluorescent probe association with a particle, except for panels where no uptake occurred.

To measure the increase in GFP-actin or rhodamine phalloidin stain at the cell cortex upon nocodazole treatment, a rectangle was drawn in ImageJ to vertically extend from outside to inside the cell cortex, and the mean fluorescence intensity was measured.

Quantitative phagocytosis assay in the presence of inhibitors of phagocytic processes

Phagocytosis assays were performed as described previously (Gilberti *et al.*, 2008) except for the addition of pharmacological inhibitors before particle addition. Briefly, cells were plated at 1×10^5 cells/cm^2 on 22-mm-square glass coverslips in 30-mm dishes and allowed to adhere overnight. Medium was replaced with 1 ml of CO_2-independent medium for 15 min and then left untreated or treated with tyrosine kinase phosphorylation inhibitor (20 µM PP2), phosphatidylinositol 3-kinase inhibitors (20 µM LY294002 or 20 nM wortmannin), actin polymerization inhibitors (500 nM latrunculin A, 500 nM latrunculin B, or 500 nM cytochalasin D), or microtubule polymerization inhibitor (800 nM nocodazole) for 45 min at 37°C in an ambient atmosphere incubator. Cells were then exposed to particles in the presence of inhibitor for 45 min before being fixed with 4% formaldehyde for 6 min at room temperature. Formaldehyde-containing medium was removed, and 1 ml of 50 mM NH_4Cl was added to quench the reaction. After fixation, the cells were stained with rabbit anti-ovalbumin antibody (Immunology Consultants Laboratory) and then fluorescein isothiocyanate–conjugated goat anti-rabbit antibody in PBS (Jackson ImmunoResearch, West Grove, PA). Particles that were opsonized with anti-ovalbumin antibody (Ab-silica and Ab-latex beads) were stained with secondary antibody only. Imaging was performed with a 63× oil immersion objective on a Zeiss Axiovert 200M microscope (Zeiss, Göttingen, Germany) using a Hamamatsu ORCA-ER camera (Hamamatsu, Bridgewater, NJ).

The surface-bound particles were counted from the fluorescence images, and the total number of particles from the DIC images. At each time point, the ratio of internalized particles to total particles was used to determine the uptake efficiency. In addition, the phagocytic index was determined as the number of internalized particles per cell per 100 macrophages. The error bars depict SE from three separate experiments.

RhoA and Rac GTPase activation

Cells were plated at 3×10^5 cells/ml in 35-mm tissue culture dishes in 1 ml of RPMI-1640 complete medium and allowed to adhere overnight, after which medium was changed to 500 µl of CO_2-independent medium for 15 min. Cells that would be exposed to COZ were treated with 100 nM PMA as previously described. All dishes were chilled on ice, and then 15 µg/cm^2 nonopsonized or Ab-opsonized 3-µm spherical silica or 8 µg/cm^2 COZ was added. The dishes were then centrifuged at 4°C at $300 \times g$ for 5 min to spin the particles onto the cells. Before placing the dishes back in the 37°C ambient air incubator, we added 500 µl of 37°C prewarmed CO_2-independent medium to the dishes to accelerate the process of warming the cells back to 37°C. Then, cells were allowed to internalize particles for 0.5, 5, 10, 15, or 30 min before samples were lysed with G-LISA lysis buffer.

Lysates were processed for the G-LISA assay according to manufacturer's guidelines (Cytoskeleton, Denver, CO). To assay for combined Rac1, 2, and 3 (referred to as Rac) or RhoA GTPase activation, 0.3 mg of total lysate, in an equal volume of binding buffer, was added in duplicate to wells of a G-LISA plate and incubated at 4°C for 30 min. The wells were washed, and anti-Rac or anti-RhoA primary antibody was added and the plate was incubated at room temperature for 45 min. The wells were then washed and incubated with horseradish peroxidase (HRP)–labeled secondary antibody for 45 min at room temperature. HRP signal was detected at 490 nm using a multiwell spectrophotometer (SpectraMax M2; Molecular Devices Sunnyvale, CA).

Measurement of endolysosomal fusion with phagosomes

Cells were plated overnight in an imaging dish as previously described. The next day, the medium was replaced with fresh RMPI-1640 complete medium containing 1 mg/ml 70-kDa tetramethylrhodamine isothiocyanate (Sigma Chemicals) or 10-kDa Texas Red (Life Technologies) dextran and incubated for 90 min at 37°C with 5% CO_2 to load the internal vesicle compartments with dextran. Medium was gently removed, and cells were washed five times with CO_2-independent medium. Once cells were on the microscope stage, particles were added to the dish and allowed to settle onto the cells. Particle types included 15 µg/cm^2 spherical silica particles, either ovalbumin coated or Ab opsonized. Cells were imaged using the Nikon A1R laser scanning confocal microscope every 30 s for at least 1 h to capture events of particle phagocytosis. The delivery of dextran to the phagosome due to fusion of endosomal and lysosomal vesicles was measured using ImageJ by outlining the vesicles containing the particle and measuring the increase in mean pixel intensity of fluorescent dextran over time. Image stacks were also converted to QuickTime movies.

Anti-tubulin immunostaining assay

Cells were plated on 22-mm glass coverslips in 35-mm tissue culture plastic dishes in 1 ml of RPMI-1640 complete medium and allowed to adhere overnight, after which medium was replaced with 1 ml of CO_2-independent medium for 15 min at 37°C in an ambient atmosphere incubator. Next cells were fixed and immunostained using a modification of the procedure of Yvon and Wadsworth (1997). Briefly, cells were fixed at room temperature for 1 min with 1 ml of 4% formaldehyde and 0.25% glutaraldehyde in PBS containing 0.1% Tween-20 (PBST). The coverslips were then further fixed with 1 ml of 4% formaldehyde and 0.25% glutaraldehyde in PHEM lysis buffer (0.5% Triton X-100, 1 mM $MgSO_4$, 5 mM ethylene glycol tetraacetic acid, and 80 mM 1,4-piperazinediethanesulfonic acid, pH 6.8) for 6 min. Next 1 ml of 50 mM NH_4Cl was added to each coverslip for 2 min to quench the reaction, and the cells were washed three times with PBST. Samples were stained with 1:10 anti-tubulin antibody (mouse monoclonal 12G10 anti–α- or E7 anti–β-tubulin; Developmental Studies Hybridoma Bank, University of Iowa, Iowa City, IA) in PBST for 30 min, washed once in PBST, and then incubated in 200 µl of 1:200 Alexa 488 goat anti-mouse antibody (Jackson ImmunoResearch) in PBST for 30 min. Samples were imaged using the Nikon A1R laser scanning confocal microscope to visualize the state of the microtubule cytoskeleton.

Detection of actin localization when microtubules are depolymerized

Cells were plated overnight in a WillCo or ibidi imaging dish and then treated with 800 nM nocodazole for 45 min in CO_2-independent medium. Cells were fixed at room temperature with 1 ml of 4%

formaldehyde and 0.25% gluteraldehyde in PBS containing 0.1% Triton X-100 and 0.1 μg/ml rhodamine phalloidin for 6 min and then imaged with a Nikon A1R laser scanning confocal microscope. To measure the increase in cortical fluorescence intensity in the presence or absence of nocodazole, the ImageJ Threshold tool was used to set maximum and minimum threshold levels so that only the phalloidin label at the cortex was highlighted and the mean fluorescence intensity of this region was measured.

Cell death assay

Cells were plated as previously described and treated with 800 nM nocodazole, 500 nM latrunculin, 500 nM cytochalasin, 20 μM LY294002, or 20 nM wortmannin in CO_2-independent medium for 45 min before particle exposure. Cells were then exposed to 15 μg/cm^2 uncoated silica particles or 40 μl of latex beads in medium containing 0.1 μg/ml propidium iodide and imaged on a widefield microscope after 0, 4, and 10 h. Approximately 300 cells, three fields of view from each time point, were scored manually for nuclear fluorescence arising from cell death.

ACKNOWLEDGMENTS

We thank Gaurav Joshi for providing the MH-S macrophage cells that stably express GFP-actin, Sergio Grinstein at the Hospital for Sick Children (Toronto, Canada) for providing the AKT-PH-GFP and 2xFYVE-GFP constructs, and Roland Wedlich-Soldner at the Max Planck Institute of Biochemistry (Munich, Germany) for the mRFP-Ruby Lifeact construct. Carol Norris at the University of Connecticut Confocal Microscopy Facility provided microscopy assistance, and we thank Sergio Grinstein, Michael Lynes, Adam Zweifach, Andrea Hubbard, and Akiko Nishiyama for many informative discussions regarding this research.

REFERENCES

Aderem A, Underhill DM (1999). Mechanisms of phagocytosis in macrophages. Annu Rev Immunol 17, 593–623.

Allen LA, Aderem A (1996). Molecular definition of distinct cytoskeletal structures involved in complement- and Fc receptor-mediated phagocytosis in macrophages. J Exp Med 184, 627–637.

Bajno L, Peng XR, Schreiber AD, Moore HP, Trimble WS, Grinstein S (2000). Focal exocytosis of VAMP3-containing vesicles at sites of phagosome formation. J Cell Biol 149, 697–706.

Bartolini F, Gundersen G (2010). Formins and microtubules. Biochim Biophys Acta 1803, 164–173.

Beamer CA, Holian A (2005). Scavenger receptor class A type I/II (CD204) null mice fail to develop fibrosis following silica exposure. Am J Physiol Lung Cell Mol Physiol 289, L186–195.

Blackford JA Jr, Antonini JM, Castranova V, Dey RD (1994). Intratracheal instillation of silica up-regulates inducible nitric oxide synthase gene expression and increases nitric oxide production in alveolar macrophages and neutrophils. Am J Respir Cell Mol Biol 11, 426–431.

Bohdanowicz M, Cosio G, Backer JM, Grinstein S (2010). Class I and class III phosphoinositide 3-kinases are required for actin polymerization that propels phagosomes. J Cell Biol 191, 999–1012.

Caron E, Hall A (1998). Identification of two distinct mechanisms of phagocytosis controlled by different Rho GTPases. Science 282, 1717–1721.

Caron E, Self AJ, Hall A (2000). The GTPase Rap1 controls functional activation of macrophage integrin alphaMbeta2 by LPS and other inflammatory mediators. Curr Biol 10, 974–978.

Castagna M, Takai Y, Kaibuchi K, Sano K, Kikkawa U, Nishizuka Y (1982). Direct activation of calcium-activated, phospholipid-dependent protein kinase by tumor-promoting phorbol esters. J Biol Chem 257, 7847–7851.

Caumont AS, Galas MC, Vitale N, Aunis D, Bader MF (1998). Regulated exocytosis in chromaffin cells. Translocation of ARF6 stimulates a plasma membrane-associated phospholipase D. J Biol Chem 273, 1373–1379.

Chao SK, Hamilton RF, Pfau JC, Holian A (2001). Cell surface regulation of silica-induced apoptosis by the SR-A scavenger receptor in a murine lung macrophage cell line (MH-S). Toxicol Appl Pharmacol 174, 10–16.

Costantini LM, Gilberti RM, Knecht DA (2011). The phagocytosis and toxicity of amorphous silica. PLoS One 6, e14647.

Cox D, Chang P, Zhang Q, Reddy PG, Bokoch GM, Greenberg S (1997). Requirements for both Rac1 and Cdc42 in membrane ruffling and phagocytosis in leukocytes. J Exp Med 186, 1487–1494.

Cox D, Tseng CC, Bjekic G, Greenberg S (1999). A requirement for phosphatidylinositol 3-kinase in pseudopod extension. J Biol Chem 274, 1240–1247.

Daeron M (1997). Fc receptor biology. Annu Rev Immunol 15, 203–234.

Damen JE, Liu L, Rosten P, Humphries RK, Jefferson AB, Majerus PW, Krystal G (1996). The 145-kDa protein induced to associate with Shc by multiple cytokines is an inositol tetraphosphate and phosphatidylinositol 3,4,5-triphosphate 5-phosphatase. Proc Natl Acad Sci USA 93, 1689–1693.

Dent EW, Gupton SL, Gertler FB (2011). The growth cone cytoskeleton in axon outgrowth and guidance. Cold Spring Harb Perspect Biol 3, a001800.

Desjardins M (1995). Biogenesis of phagolysosomes: the "kiss and run" hypothesis. Trends Cell Biol 5, 183–186.

Duclos S, Corsini R, Desjardins M (2003). Remodeling of endosomes during lysosome biogenesis involves "kiss and run" fusion events regulated by rab5. J Cell Sci 116, 907–918.

Fitzer-Attas CJ, Lowry M, Crowley MT, Finn AJ, Meng F, DeFranco AL, Lowell CA (2000). Fcgamma receptor-mediated phagocytosis in macrophages lacking the Src family tyrosine kinases Hck, Fgr, and Lyn. J Exp Med 191, 669–682.

Fubini B (1998). Surface chemistry and quartz hazard. Ann Occup Hyg 42, 521–530.

Ghazizadeh S, Bolen JB, Fleit HB (1994). Physical and functional association of Src-related protein tyrosine kinases with Fc gamma RII in monocytic THP-1 cells. J Biol Chem 269, 8878–8884.

Gilberti RM, Joshi GN, Knecht DA (2008). The phagocytosis of crystalline silica particles by macrophages. Am J Respir Cell Mol Biol 39, 619–627.

Gordon S (1995). The macrophage. Bioessays 17, 977–986.

Greenberg S, Grinstein S (2002). Phagocytosis and innate immunity. Curr Opin Immunol 14, 136–145.

Griffin FM Jr, Griffin JA, Silverstein SC (1976). Studies on the mechanism of phagocytosis. II. The interaction of macrophages with anti-immunoglobulin IgG-coated bone marrow-derived lymphocytes. J Exp Med 144, 788–809.

Gu H, Botelho RJ, Yu M, Grinstein S, Neel BG (2003). Critical role for scaffolding adapter Gab2 in Fc gamma R-mediated phagocytosis. J Cell Biol 161, 1151–1161.

Haberzettl P, Duffin R, Kramer U, Hohr D, Schins RP, Borm PJ, Albrecht C (2007). Actin plays a crucial role in the phagocytosis and biological response to respirable quartz particles in macrophages. Arch Toxicol 81, 459–470.

Hackam DJ, Rotstein OD, Schreiber A, Zhang W, Grinstein S (1997). Rho is required for the initiation of calcium signaling and phagocytosis by Fcgamma receptors in macrophages. J Exp Med 186, 955–966.

Hall AB, Gakidis MA, Glogauer M, Wilsbacher JL, Gao S, Swat W, Brugge JS (2006). Requirements for Vav guanine nucleotide exchange factors and Rho GTPases in FcgammaR- and complement-mediated phagocytosis. Immunity 24, 305–316.

Hamilton R, de Villiers WJS, Holian A (2000). Class A type II scavenger receptor mediates silica-induced apoptosis in Chinese hamster ovary cell line. Toxicol Appl Pharmacol 162, 100–106.

Hamilton RF Jr, Thakur SA, Mayfair JK, Holian A (2006). MARCO mediates silica uptake and toxicity in alveolar macrophages from C57BL/6 mice. J Biol Chem 34218–34226.

Hanke JH, Gardner JP, Dow RL, Changelian PS, Brissette WH, Weringer EJ, Pollok BA, Connelly PA (1996). Discovery of a novel, potent, and Src family-selective tyrosine kinase inhibitor. Study of Lck- and FynT-dependent T cell activation. J Biol Chem 271, 695–701.

Honda A, Nogami M, Yokozeki T, Yamazaki M, Nakamura H, Watanabe H, Kawamoto K, Nakayama K, Morris AJ, Frohman MA, Kanaho Y (1999). Phosphatidylinositol 4-phosphate 5-kinase alpha is a downstream effector of the small G protein ARF6 in membrane ruffle formation. Cell 99, 521–532.

Huaux F (2007). New developments in the understanding of immunology in silicosis. Curr Opin Allergy Clin Immunol 7, 168–173.

Indik Z, Kelly C, Chien P, Levinson AI, Schreiber AD (1991). Human Fc gamma RII, in the absence of other Fc gamma receptors, mediates a phagocytic signal. J Clin Invest 88, 1766–1771.

Iyer R, Hamilton RF, Li L, Holian A (1996). Silica-induced apoptosis mediated via scavenger receptor in human alveolar macrophages. Toxicol Appl Pharmacol 141, 84–92.

Iyer R, Holian A (1997). Involvement of the ICE family of proteases in silica-induced apoptosis in human alveolar macrophages. Am J Physiol 273, L760–L767.
Joshi GN, Knecht DA (2013). Silica phagocytosis causes apoptosis and necrosis by different temporal and molecular pathways in alveolar macrophages. Apoptosis 18, 271–285.
Kiefer F, Brumell J, Al-Alawi N, Latour S, Cheng A, Veillette A, Grinstein S, Pawson T (1998). The Syk protein tyrosine kinase is essential for Fcgamma receptor signaling in macrophages and neutrophils. Mol Cell Biol 18, 4209–4220.
Kobzik L (1995). Lung macrophage uptake of unopsonized environmental particulates. Role of scavenger-type receptors. J Immunol 155, 367–376.
Lee CY, Herant M, Heinrich V (2011). Target-specific mechanics of phagocytosis: protrusive neutrophil response to zymosan differs from the uptake of antibody-tagged pathogens. J Cell Sci 124, 1106–1114.
Lewkowicz E, Herit F, Le Clainche C, Bourdoncle P, Perez F, Niedergang F (2008). The microtubule-binding protein CLIP-170 coordinates mDia1 and actin reorganization during CR3-mediated phagocytosis. J Cell Biol 183, 1287–1298.
Loijens JC, Boronenkov IV, Parker GJ, Anderson RA (1996). The phosphatidylinositol 4-phosphate 5-kinase family. Adv Enzyme Regul 36, 115–140.
Machesky LM, Insall RH (1999). Signaling to actin dynamics. J Cell Biol 146, 267–272.
Marshall JG, Booth JW, Stambolic V, Mak T, Balla T, Schreiber AD, Meyer T, Grinstein S (2001). Restricted accumulation of phosphatidylinositol 3-kinase products in a plasmalemmal subdomain during Fc gamma receptor-mediated phagocytosis. J Cell Biol 153, 1369–1380.
May RC, Caron E, Hall A, Machesky LM (2000). Involvement of the Arp2/3 complex in phagocytosis mediated by FcγR or CR3. Nat Cell Biol 2, 246–248.
May RC, Machesky LM (2001). Phagocytosis and the actin cytoskeleton. J Cell Sci 114, 1061–1077.
Newman SL, Mikus LK, Tucci MA (1991). Differential requirements for cellular cytoskeleton in human macrophage complement receptor- and Fc receptor-mediated phagocytosis. J Immunol 146, 967–974.
Palecanda A, Kobzik L (2001). Receptors for unopsonized particles: the role of alveolar macrophage scavenger receptors. Curr Mol Med 1, 589–595.
Patel PC, Harrison RE (2008). Membrane ruffles capture C3bi-opsonized particles in activated macrophages. Mol Biol Cell 19, 4628–4639.
Pitt A, Mayorga LS, Stahl PD, Schwartz AL (1992). Alterations in the protein composition of maturing phagosomes. J Clin Invest 90, 1978–1983.
Riedl J, Crevenna AH, Kessenbrock K, Yu JH, Neukirchen D, Bista M, Bradke F, Jenne D, Holak TA, Werb Z, *et al.* (2008). Lifeact: a versatile marker to visualize F-actin. Nat Methods 5, 605–607.
Scott CC, Botelho RJ, Grinstein S (2003). Phagosome maturation: a few bugs in the system. J Membr Biol 193, 137–152.
Scott CC, Dobson W, Botelho RJ, Coady-Osberg N, Chavrier P, Knecht DA, Heath C, Stahl P, Grinstein S (2005). Phosphatidylinositol-4,5-bisphosphate hydrolysis directs actin remodeling during phagocytosis. J Cell Biol 169, 139–149.
Shen HM, Zhang Z, Zhang QF, Ong CN (2001). Reactive oxygen species and caspase activation mediate silica-induced apoptosis in alveolar macrophages. Am J Physiol Lung Cell Mol Physiol 280, L10–L17.
Shi Y, Tohyama Y, Kadono T, He J, Miah SM, Hazama R, Tanaka C, Tohyama K, Yamamura H (2006). Protein-tyrosine kinase Syk is required for pathogen engulfment in complement-mediated phagocytosis. Blood 107, 4554–4562.
Stenmark H, Gillooly DJ (2001). Intracellular trafficking and turnover of phosphatidylinositol 3-phosphate. Semin Cell Dev Biol 12, 193–199.
Suzuki T, Kono H, Hirose N, Okada M, Yamamoto T, Yamamoto K, Honda Z (2000). Differential involvement of Src family kinases in Fc gamma receptor-mediated phagocytosis. J Immunol 165, 473–482.
Swanson JA, Baer SC (1995). Phagocytosis by zippers and triggers. Trends Cell Biol 5, 89–93.
Taylor PR, Martinez-Pomares L, Stacey M, Lin HH, Brown GD, Gordon S (2005). Macrophage receptors and immune recognition. Annu Rev Immunol 23, 901–944.
Thakur SA, Beamer CA, Migliaccio CT, Holian A (2009). Critical role of MARCO in crystalline silica-induced pulmonary inflammation. Toxicol Sci 108, 462–471.
Thibodeau M, Giardina C, Hubbard AK (2003). Silica-induced caspase activation in mouse alveolar macrophages is dependent upon mitochondrial integrity and aspartic proteolysis. Toxicol Sci 76, 91–101.
Thibodeau MS, Giardina C, Knecht DA, Helble J, Hubbard AK (2004). Silica-induced apoptosis in mouse alveolar macrophages is initiated by lysosomal enzyme activity. Toxicol Sci 80, 34–48.
Tjelle TE, Lovdal T, Berg T (2000). Phagosome dynamics and function. Bioessays 22, 255–263.
Toker A, Cantley LC (1997). Signalling through the lipid products of phosphoinositide-3-OH kinase. Nature 387, 673–676.
Vallyathan V, Shi X (1997). The role of oxygen free radicals in occupational and environmental lung diseases. Environ Health Perspect 105(Suppl 1), 165–177.
Varnai P, Balla T (1998). Visualization of phosphoinositides that bind pleckstrin homology domains: calcium- and agonist-induced dynamic changes and relationship to myo-[3H]inositol-labeled phosphoinositide pools. J Cell Biol 143, 501–510.
Vieira OV, Botelho RJ, Grinstein S (2002). Phagosome maturation: aging gracefully. Biochem J 366, 689–704.
Vieira OV, Botelho RJ, Rameh L, Brachmann SM, Matsuo T, Davidson HW, Schreiber A, Backer JM, Cantley LC, Grinstein S (2001). Distinct roles of class I and class III phosphatidylinositol 3-kinases in phagosome formation and maturation. J Cell Biol 155, 19–25.
Vieira OV, Bucci C, Harrison RE, Trimble WS, Lanzetti L, Gruenberg J, Schreiber AD, Stahl PD, Grinstein S (2003). Modulation of Rab5 and Rab7 recruitment to phagosomes by phosphatidylinositol 3-kinase. Mol Cell Biol 23, 2501–2514.
Yeung T, Ozdamar B, Paroutis P, Grinstein S (2006). Lipid metabolism and dynamics during phagocytosis. Curr Opin Cell Biol 18, 429–437.
Yvon AM, Wadsworth P (1997). Non-centrosomal microtubule formation and measurement of minus end microtubule dynamics in A498 cells. J Cell Sci 110, 2391–2401.
Zhou Q, Kee YS, Poirier CC, Jelinek C, Osborne J, Divi S, Surcel A, Will ME, Eggert US, Muller-Taubenberger A, *et al.* (2010a). 14–3-3 coordinates microtubules, Rac, and myosin II to control cell mechanics and cytokinesis. Curr Biol 20, 1881–1889.
Zhou J, Kim HY, Wang JH, Davidson LA (2010b). Macroscopic stiffening of embryonic tissues via microtubules, RhoGEF and the assembly of contractile bundles of actomyosin. Development 137, 2785–2794.